Eur. Phys. J. B **6**, 45–55 (1998)

THE EUROPEAN PHYSICAL JOURNAL B

Adsorption kinetics of a bidisperse polymer solution

J. Baschnagel[a], A. Johner[b], and J.-F. Joanny

Institut Charles Sadron[c], 6 rue Boussingault, 67083 Strasbourg Cedex, France

Received: 5 November 1997 / Revised: 15 April 1998 / Accepted: 8 July 1998

Abstract. We consider the competitive adsorption of a bidisperse polymer solution of long and short chains onto a flat surface. Starting from an adsorbed layer, mainly formed by short chains, the replacement of short by long chains is studied for fixed and very dilute bulk concentration. Our theory is restricted to the case of weak, reversible adsorption, where the net monomer-surface contact energy is much smaller than the thermal energy. We obtain the following description of the replacement process. After a fast first step which depends on the initial composition of the layer, the structure of the layer changes in a universal way: First, long and short chains are exchanged at almost constant layer thickness until most of the short chains have been replaced. Then, the layer's thickness rapidly grows and saturates at the final equilibrium value. In equilibrium the layer predominantly consists of long chains.

PACS. 68.10.Jy Kinetics (evaporation, adsorption, condensation, catalysis, etc.) – 82.65.Dp Thermodynamics of surfaces and interfaces – 61.25.Hq Macromolecular and polymer solutions; polymer melts; swelling

1 Introduction

The adsorption onto a solid surface from fairly monodisperse polymer solutions has been studied by both theory and experiments [1,2]. Experiments reveal that there are two limiting situations: reversible and (almost) irreversible adsorption. Irreversible adsorption occurs when the contact energy between a monomer and the surface is larger than the thermal energy k_BT. Such a situation is realized, for instance, for the adsorption of poly(methyl methacrylate) (PMMA) from a carbon tetrachloride (CCl_4) solution onto oxidized silicon. In this system strong hydrogen bonds lead to a net monomer-surface interaction of about $4k_BT$ [3]. If adsorption takes place from dilute solution, the chains, which first arrive at the bare surface, quickly spread to maximize the number of contacts and adopt a flattened configuration. They remain in this configuration as the surface coverage increases so that late arriving chains only find few sites to adsorb and are bound loosely. The resulting distribution of chain configurations is bimodal and therefore far from that expected in equilibrium [3].

Similar observations were also made in other systems, where the monomer-surface energy is smaller. In pioneering experiments Pefferkorn *et al.* [4] studied the adsorption of polystyrene (PS) onto silica beads from CCl_4 (contact energy $\simeq 1k_BT$ [5]) and discovered at moderate dilution a long-lived metastable bimodal distribution of irreversibly and reversibly (though strongly) bound chains. Since then, extensive work has confirmed the essential correctness of this result [6–8].

In spite of much effort, a convincing theoretical description of these non-equilibrium systems is not available, except for the so-called "pseudo-brush". The pseudo-brush is a paradigm for a metastable layer configuration. It forms if a strongly binding system, such as poly(dimethyl siloxane) from toluene onto silica, adsorbs first from concentrated solution, and if the solution is then replaced by pure solvent. The adsorption from concentrated solution leads to a high adsorbance, Γ, of order $\Gamma \sim R\phi_0$, where R and ϕ_0 are the radius of gyration and the monomer volume fraction in the bulk, respectively. The subsequent swelling in pure solvent makes the polymers stretch away from the surface to accomodate the high adsorbance. Thus a (highly polydisperse) brush-like structure forms, which was first described by Guiselin [9]. During the swelling the adsorbance is almost quenched because desorption involves the release of many monomer-wall contacts, which is energetically very unfavorable. Thus metastable states related to very slow chain desorption will be predicted by any theory (including equilibrium theory). A test of Guiselin's predictions about the structure of the pseudo-brush was attempted in a recent Monte-Carlo simulation [10]. However, the chain lengths studied were too short to distinguish unambiguously between the pseudo-brush picture and the self-similar structure of weakly adsorbed chains [11–13].

[a] *Present address:* Institut für Physik, Universität Mainz, Staudinger Weg 7, 55099 Mainz, Germany.
[b] e-mail: `johner@ics-crm.u-strasbg.fr`
[c] UPR CNRS 022.

In order to approach the problem of the desorption kinetics in strongly adsorbing systems Douglas *et al.* [14] and Johnson *et al.* [15] suggested that it is not the energetics of the surface detachment, but rather the sluggish diffusion out of the layer that is rate-limiting. Based on this idea they predict that the adsorbance should exhibit a stretched-exponential time dependence with a stretching exponent of 1/2, and that the desorption time should scale with chain length as the diffusion coefficient. Whereas these expectations were confirmed in experiments, where PMMA replaces PS previously adsorbed on oxidized silicon [15], a weaker displacer, deuterio-*cis*-polyisoprene (contact energy $\simeq 3k_BT$) yielded considerable deviations [7].

Another sometimes proposed idea is to compare the properties of strongly adsorbing chains with the random sequential adsorption of mutually excluding disks or spheres [6]. However, such an analogy seems questionable because already a swollen polymer of chain length N, spread over its bulk radius R, only represents a surface density of $\sim N/R^2 \sim N^{-1/5}$, which vanishes in the limit of infinitely long chains. If the chain distorts during spreading to increase the number of surface contacts, one can expect that the area occupied by a chain is even less densely covered and thus not completely blocked, as it is assumed in the analogy to hard disks.

The selection of theoretical explanations presented above, which work for some but not all systems, illustrates how difficult it is to develop an adequate description of strong adsorption. This is due to the non-equilibrium nature of the processes involved, which resemble, in some aspects, those of glassy materials. A complete understanding of these strongly site-binding systems seems to be as intricate as that of glasses in general.

Therefore we focus on reversible (monomer) adsorption in the following. Reversible adsorption occurs when a chain adsorbs strongly due to many surface contacts, although the net energy gain of an individual monomer is much smaller than k_BT. This idea underlies most of the theories for the structure of the adsorption layer proposed so far [1,2,12,13,16,17], and an early kinetic study by de Gennes which addresses adsorption, desorption and labeled/unlabeled chain exchange [18]. If the energy gain of a monomer is small, the local relaxation of the layer structure (*i.e.*, the distributions of trains, loops and tails) is fairly fast. One can then assume that the layer quickly equilibrates on the time scale of the processes considered. In fact, when the layer is exposed to pure solvent, chain desorption turns out to be a very slow process [8,19]. It is so slow because the desorption requires the simultaneous release of all anchored monomers, which is energetically very unfavorable. More probable is a monomer-by-monomer replacement process, as could occur during the exchange of chains from the layer and the bulk. This exchange was first studied experimentally for poly(acryl amide) adsorbed from water onto aluminosilicate beads [19]. At the beginning a layer of tritium-labeled polymer was formed. Then the solution was replaced by unlabeled, but otherwise identical chains, and the exchange was observed. The exchange proceeded at constant surface coverage, with rate proportional to the bulk concentration, and it was considerably faster than the desorption in pure solvent.

A similar situation could be expected for the competitive adsorption of a bidisperse polymer mixture. This is binary mixture of two chemically identical chains, which differ only in length. In thermal equilibrium both experiments [1,5,20,21] and theory [22,23] show that the long species is preferentially adsorbed from dilute solution. However, during the initial stages of adsorption the layer mainly consists of short chains. Therefore, there has to be an intermediate time regime, where short chains are exchanged by longer ones. This is clearly seen in experiments by Dijt *et al.* [5]. One of these experiments employed poly(ethylene oxide) (PEO) adsorbed from water onto silica (in the form of an oxidized silicon wafer [20]) and gave the following results:

- short chains reach the wall first and determine the initial increase of adsorbance,
- the final equilibrium state is dominated by the long chains,
- the total adsorbance reaches a pseudo-plateau at intermediate times (without exhibiting an overshoot, which would be a signal of non-equilibrium adsorption). This plateau essentially coincides with the equilibrium adsorbance of the short chains in the absence of the longer species. The plateau is related to the exchange of small chains,
- the adsorbance remains nearly constant until the exchange is almost complete. The exchange is fast: it proceeds over less than a minute.

Dijt *et al.* rationalize their findings by the assumption that the adsorbed layer is in thermal equilibrium at every time instant of the exchange process, and they support their interpretation by a numerical calculation of the adsorption isotherm with the Scheutjens-Fleer theory [1]. Similar conclusions where reached by Maria Santore very recently [24].

The Scheutjens-Fleer theory quantitatively agrees with a recently developed extended mean-field theory for the adsorption of both monodisperse [13] and bidisperse chains [23]. The extended mean-field theory goes beyond the so-called "ground-state dominance approximation" [1] by calculating the contribution of the tails to thermodynamic properties of the layer. A tail is a portion of an adsorbed chain, which touches the surface only by its first monomer, whereas all remaining monomers dangle into the solution. These dangling monomers swell the layer. In the limit of infinite chain length and vanishing concentration (standard ground-state approximation) the contribution of the tails vanishes. All monomers are then bound in "loops". A loop is part of a chain in which the first and the last monomer touch the surface. By taking tails into account the mean-field theory is therefore extended to finite chain lengths.

In addition to mean-field theory a corresponding scaling theory was also developed to treat good solvent conditions [12,23]. The purpose of the present paper is to apply

the results of this scaling approach to derive the two-step behavior of the adsorbance for the competitive adsorption of a bidisperse polymer mixture and to provide an analytical explication of the experiment described above.

The remainder of the paper is organized as follows: in Section 2 we gather those results of previous publications [12,23,25] which are necessary for the subsequent calculations. We first describe the structure of the adsorbed layer in thermal equilibrium with a dilute bulk solution, examine the rate limiting processes and derive the kinetic equations. This discussion will deal with a monodisperse solution only. In Section 3 we generalize these results to the bidisperse case and solve the rate equations. The last section summarizes the main points of our work and discusses the relevance of our results for experiments.

2 The adsorption rate limiting processes and the kinetic laws

Consider a dilute solution of a polymer with chain length N. For the solution to be dilute the volume fraction, ϕ_0, of the monomers (in the bulk) has to be smaller than the overlap concentration $\phi^* \sim N^{1-3\nu}$, where ν is the (critical) exponent relating the radius of gyration, R, to the chain length by $R \sim N^\nu$. Under good solvent conditions it has the value $\nu \approx 0.59$.

This solution is now exposed to an impenetrable wall which is assumed to exert a short-range attraction on all monomers and to be structureless in the x, y directions. Therefore the distance to the wall, z, is the only relevant coordinate. A monomer touching the wall gains an energy $\delta \ll k_BT$, where the critical contact energy at the adsorption threshold (which is of order k_BT) has been subtracted. Due to the fast monomer adsorption/desorption at the wall the relevant energy is the difference, ϵ, between the chemical potentials of a free monomer in the bulk and a monomer belonging to a sequence of short loops at the wall. It depends on chain length and volume fraction [12]. In the plateau regime, where the layer is continuous, ϵ has a much smaller value than the monomer-surface contact energies quoted in the introduction [13]. Since we want to treat the case of reversible adsorption, we assume that a chain is strongly bound at the wall due to many monomer contacts, whereas the energy gain per monomer is small. This implies that $\epsilon \ll k_BT$, but $N\epsilon \gg k_BT$. This criterion is easily satisfied in the plateau regime, but much more restrictive during the early stages of adsorption, in the dilute surface regime where the surface is hardly covered.

During the early stages of its adsorption an incoming chain is very likely to desorb because only few monomers touch the wall. However, if a critical number of monomers, G, is adsorbed, desorption becomes suppressed. G is given by $G\epsilon \simeq k_BT$. On the other hand, G can also be interpreted as the maximum number of monomers in a loop or a tail that the thermal energy succeeds in releasing from the wall for a given ϵ. Therefore, G determines the size, λ, of the adsorbed layer by $\lambda \sim G^\nu$. Since $G \simeq k_BT/\epsilon$, λ is inversely proportional to a power of the contact energy (this only makes sense as long as $\epsilon < k_BT$). Physically, such a relationship is sensible. The larger the energy gain of a monomer, the more tightly a chain is bound to the wall and the smaller the extension of the layer into the bulk becomes. Furthermore, the assumption that a chain is strongly adsorbed ($N\epsilon \gg k_BT$) immediately implies that $R \gg \lambda$.

In addition to λ the previous analysis in terms of loops and tails [12,13] showed that there exists another characteristic length scale, $z^* \sim N^{1/2}$, in the adsorbed layer, which divides the layer into two regions: an inner region close to the wall ($0 < z < z^*$) and an outer region further away from it ($z^* < z < \lambda$). In the inner region the concentration of the tails is very small so that the loops essentially determine the structure of the layer, whereas it is exactly vice versa in the outer region.

However, the two length scales, z^* and λ, are not always well separated. Since $z^*/\lambda \sim N^{-1/10}$ only, the prefactors of the scaling laws become important for finite chain length. They depend on the bulk concentration and adsorption strength, and can be calculated exactly in mean-field theory. A detailed comparison of the mean-field theory with the Scheutjens-Fleer theory [13] showed that z^* is almost independent of concentration for dilute solution, whereas λ decreases strongly upon dilution. For strong dilution and typical experimental chain lengths z^* becomes larger than λ, and tails dominate only in the distal region, *i.e.*, for $z > \lambda$ [13]. Therefore we want to focus our study on this so-called "starved regime", where $z^* > \lambda$.

In the starved regime the classical analogy of the concentration profiles to critical phenomena [11] holds everywhere inside the layer. The monomer volume fraction, $\phi(z)$, and the end-monomer volume fraction, $\phi_e(z)$, decay as power laws [12]

$$\phi(z) \sim z^{-3+1/\nu} \quad \text{and} \quad \phi_e(z) \sim z^{-\beta/\nu} , \tag{1}$$

where $\beta \approx 0.30$ and $\nu \approx 0.59$ [26]. From $\phi_e(z)$ the partition function of a tail, $Z_t(n)$, with n monomers can be calculated. Due to the self-similar structure of the concentration profile a tail at position z has $n \sim z^{1/\nu}$ monomers so that

$$Z_t(n) \sim \phi_e(z)\frac{dz}{dn} \sim n^{(\gamma-\nu)/2-1} , \tag{2}$$

where the relation, $\gamma = 3\nu - 2\beta \approx 1.16$, between the critical exponents was used [26]. Using this partition function the adsorbance, Γ, of the layer in thermal equilibrium with the bulk solution can be estimated by balancing the respective chemical potentials. The bulk concentration of free indistinguishable self-avoiding chains is ϕ_0/N so that

$$\frac{\mu_b}{k_BT} = \frac{\mu_{b,m}}{k_BT} + \frac{1}{N}\ln\frac{\phi_0}{N} - \frac{1}{N}\ln N^{\gamma-1} . \tag{3}$$

The first term stems from the partition function of a monomer, the second accounts for the entropy of mixing, and the last one results from the enhancement factor of the partition function of a single self-avoiding chain. On the other hand, the surface concentration of indistinguishable self-avoiding chains in the interfacial layer is Γ/N.

Each of the chains has two tails and an unknown number of loops. Due to this unknown number the chemical potential of the adsorbed layer is more difficult to estimate than that of the bulk. A possible reasoning runs as follows: Since the layer is rather dense close to the wall, one can assume that the (small) loops behave as if they formed a two-dimensional melt [12,27]. For a two-dimensional melt $\nu = 1/2$, but the exponent γ takes the non-trivial value $\gamma_{2D} = 19/16 \approx 1.19$ [28]. The contribution of the loops to the chemical potential is then in analogy to equation (3)

$$\frac{\mu_{a,loop}}{k_BT} \approx \frac{\mu_{a,m}}{k_BT} + \frac{1}{N}\ln\frac{\Gamma}{N} - \frac{1}{N}\ln N^{\gamma_{2D}-1} , \qquad (4)$$

and that of the two tails is given by

$$\frac{\mu_{a,tail}}{k_BT} \simeq -\frac{1}{N}\ln\left[\int_0^G Z_t(n)dn\right]^2 = -\frac{1}{N}\ln\left[\frac{G^{\gamma-\nu}}{C}\right] , \qquad (5)$$

where C is a constant of order unity. Adding both contributions and imposing $\mu_a = \mu_b$ we find

$$\Gamma = \frac{\phi_0}{C} N^{\gamma_{2D}-\gamma} G^{\gamma-\nu} \exp\left[\frac{N}{G}\right] , \qquad (6)$$

where the adsorption energy is $\epsilon = \mu_{b,m} - \mu_{a,m} = k_BT/G$.

Based on these static results the dynamics of the adsorption process can now be considered. The adsorbance, Γ, changes with time because adsorbed chains desorb and free chains from the bulk adsorb. The desorbing chains create an outward flux, J_{out}, which competes with the inward flux, J_{in}, of the adsorbing chains. This yields

$$\frac{d\Gamma}{dt} = J_{in} - J_{out} . \qquad (7)$$

Quite generally, a flux is given by the ratio of a concentration and a resistance K (inverse velocity). For the incoming flux the concentration (volume fraction) is equal to the (constant) monomer volume fraction in the bulk so that

$$J_{in} = \frac{\phi_0}{K} . \qquad (8)$$

On the other hand, the concentration for the outward flux is determined by the instantaneous monomer volume fraction in the changing adsorbed layer. To calculate J_{out}, we invoke a local equilibrium assumption which is justified if the relaxation time of the layer is much smaller than all pertinent time scales of the adsorption process. This is the case in the above mentioned experiments with PEO [5,20] and seems reasonable in dilute solutions, since the longest relaxation time of the adsorbed chains is smaller than the Rouse time $\sim \zeta_0 N^2$ (if Rouse dynamics is assumed) and (in any case) independent of the bulk concentration, whereas the typical time scales of the adsorption kinetics are inversely proportional to concentration [25]. Then J_{out} is given by an equation similar to equation (8) with ϕ replaced by the (hypothetical) concentration that the bulk solution must have to be in equilibrium with a layer of (instantaneous) size G. This concentration is determined by equation (6), and so

$$J_{out} = \frac{C\Gamma}{K} N^{\gamma-\gamma_{2D}} G^{\nu-\gamma} \exp\left[-\frac{N}{G}\right] . \qquad (9)$$

The resistance, K, characterizes the barrier, built up by the adsorbed layer, that incoming chains have to overcome. This barrier consists of two parts: an up-hill part for the chain penetration and a down-hill part for the spreading of the chain on the wall. Using asymptotic scaling laws both processes have recently been studied in detail [25]. Two penetration mechanisms were identified: end and hairpin penetration. Hairpin penetration occurs when a central monomer rather than a monomer close to the chain end touches the wall first. For a starved layer it turns out that this is the fastest penetration mechanism. Physically, this result is reasonable. If the statistical coil of a free bulk chain arrives at the layer, it is much more likely that it impinges with an inner than with an end monomer. This impingement can lead to penetration because the starved layer is rather porous and thus transparent for incoming chains.

As soon as the first monomer touches the wall, the chain reaches the activated state for the subsequent spreading along the surface [25]. The activated state corresponds to the top of the energy barrier against adsorption. This energy barrier is larger than k_BT (see below), and thus the chain is most likely to desorb again. The heuristic explanation for this result is that a monomer only gains the small energy $\epsilon \ll k_BT$ upon adsorption. Therefore thermal fluctuations can easily cause desorption during the early stages of spreading. As more and more monomers find their places at the surface, the probability of desorption decreases, until it becomes effectively suppressed when the critical number of monomers, G, is adsorbed. Since the energy of the activated state is larger than k_BT, we can use Kramers rate theory to determine the resistance. For a starved layer, spreading is the rate limiting process (see discussion below and Ref. [25]). The resistance is then given by [25]

$$K = \int_0^G \frac{\exp[U(n)/k_BT]}{D} dn , \qquad (10)$$

where $U(n)$ is the energy needed to spread n monomers of the incoming chain on the wall, and D is the monomeric diffusion constant for the spreading process.

To estimate D we assume Rouse dynamics. In this case, both the direct friction and the friction due to the in-plane expulsion of already adsorbed monomers are of the order of a monomer friction ζ_0. The relevant diffusion constant is then $D \sim k_BT/\zeta_0$.

The energy $U(n)$ can be calculated from the partition function, $Z(n)$, of a hairpin configuration with n monomers spread on the wall,

$$\exp\left[-\frac{U(n)}{k_BT}\right] = \frac{Z(n)}{Z_0} , \qquad (11)$$

where $Z_0 \sim N^{\gamma-1}$ is the partition function of a chain in the bulk. $Z(n)$ is the product of two factors [25]: the partition function Z_s of the n monomers at the surface and that of the two long tails, which is identical to the partition function, Z_{as}, of a hairpin in the activated state (as). The hairpin contribution is obtained from the following scaling argument [25]. If $N \simeq G$, $Z_{as} = GZ_t^2(G)$, where the extra factor G takes into account that any of the $\sim G$ central monomers may be in contact with the surface. If $N \gg G$, the chain may be considered, on large scales, as a chain being attached to an impenetrable wall by any of its inner monomers. As there is no special surface exponent for the partition function in this case [28], Z_{as} scales with the overall chain length as $N^{\gamma-1}$. An interpolation between these two limiting cases with a power law yields [25]

$$Z_{as} \sim \left(\frac{N}{G}\right)^{\gamma-1} GZ_t^2(G) \overset{(2)}{\sim} N^{\gamma-1}G^{-\nu} \qquad (12)$$

so that $U_{as}/k_BT \sim \ln G^{\nu} > 1$, as anticipated above. To calculate the factor $Z_s(n)$ we assume, as before, that the structure of the n adsorbed monomers resembles a two-dimensional melt [25]. Then Z_s is the product of the enhancement factor $n^{\gamma_{2D}-1}$ and of the nth power of the monomer partition function. Since the latter partition function is $\exp[\epsilon/k_BT]$, we find

$$Z_s(n) \sim n^{\gamma_{2D}-1} \exp\left[\frac{n\epsilon}{k_BT}\right] . \qquad (13)$$

Multiplying equations (12, 13) we obtain the partition function of a hairpin,

$$Z(n) \sim N^{\gamma-1}n^{\gamma_{2D}-1}G^{-\nu} \exp\left[\frac{n}{G}\right] , \qquad (14)$$

and from that and equations (10, 11) the resistance

$$K \simeq \frac{\zeta_0}{k_BT}G^{2-\gamma_{2D}+\nu} . \qquad (15)$$

Using equations (8, 9, 15) the inward and outward fluxes read

$$J_{in} = \frac{k_BT}{\zeta_0}\phi_0 G^{-(2-\gamma_{2D}+\nu)} \qquad (16)$$

and

$$J_{out} = \frac{k_BT}{\zeta_0}C\Gamma N^{\gamma-\gamma_{2D}}G^{\gamma_{2D}-\gamma-2} \exp\left[-\frac{N}{G}\right] . \qquad (17)$$

So far we have neglected the bulk diffusion. In practice, the depleted diffusion layer has a hydrodynamic thickness L which is fixed by the convection in the bulk solution and usually does not exceed 1 μm. L defines an upper bound $K_D \sim \eta_s LR/k_BT$ for the diffusion resistance where the monomer friction in the pure solvent $\zeta_s \sim 6\pi\eta_s a$ can be different from the wall friction ζ_0. Comparing the diffusion and the spreading resistance we find: $K/K_D = (\zeta_0/\zeta_s)\,(G/G^{\star})^{2-\gamma_{2D}+\nu}\,(R/L)$ with $G^{\star} \sim N^{2\nu/(2-\gamma_{2D}+\nu)}$. If $G \sim G^{\star} \sim N^{0.84}$, ζ_0 must overcome ζ_s by one or two orders of magnitude for the spreading process to be rate limiting at any time. From an experimental point of view this is not unreasonable because it is sometimes even found that the surface layer behaves almost glass-like. Although the freezing-in of the surface layer would be promoted by strong monomer binding in a rugged surface potential, the high densities achieved close to the surface, even in a weak surface potential, should be enough to slow down the spreading dynamics. The assumption of Rouse dynamics certainly underestimates the friction during the spreading process. The friction should increase by the formation of entanglements, which would also lead to a different (stonger) dependence of the resistance on the layer thickness. Entanglements should thus favor spreading as the rate-controling step. We therefore believe that our analysis, though initially based on Rouse dynamics, yields a qualitatively correct description of the adsorption kinetics if formulated in quite general terms, as is done below.

When bulk diffusion is rate limiting, a case we do not want to consider in detail, the diffusion length corresponding to an appreciable variation of the partial adsorbance, is $\sim \Gamma/\phi_0$. At high dilution the diffusion resistance is thus controlled by the hydrodynamic thickness. Such a regime could be described in the framework of the present theory with $\mu = 0$ in equation (25) and a rescaling of the equations different from that proposed below. In the following we assume that spreading is the rate limiting step due to the reasons discussed above.

Equations (7, 16, 17) define our approach to the adsorption kinetics for a starved layer. For the subsequent discussion of the competitive adsorption of a bidisperse mixture, two time scales of the monodisperse case are important: the adsorption time τ_a and the exchange time, τ_{ex}, of already adsorbed chains by free chains from the bulk [25]. To find τ_a it is convenient to introduce the undersaturation

$$X = \Gamma_{\infty} - \Gamma , \qquad (18)$$

where Γ_{∞} is the equilibrium value of Γ for infinitely long chains. The integration of the concentration profile, $\phi(z)$, (see Eq. (1)) yields

$$X \sim G^{1-2\nu} . \qquad (19)$$

At the early stages of the adsorption process, $N \gg G(t)$, so that J_{out} is exponentially small (see Eq. (17)) and can be neglected in comparison with J_{in}. Inserting the undersaturation X in equations (7, 16) the rate equation becomes

$$\frac{dX}{dt} \sim -\frac{k_BT}{\zeta_0}\phi_0 X^{-(2-\gamma_{2D}+\nu)/(1-2\nu)} , \qquad (20)$$

which leads to

$$t(G) \sim \frac{\zeta_0}{\phi_0 k_BT}G^{3-\gamma_{2D}-\nu} . \qquad (21)$$

In analogy to reference [25] we define τ_a as time needed to form a layer of thickness $G \sim N$, *i.e.*,

$$\tau_a \sim \frac{\zeta_0}{\phi_0 k_B T} N^{3-\gamma_{2D}-\nu} . \quad (22)$$

The second important time scale is the exchange time of adsorbed chains against free chains, if the layer is in thermal equilibrium with the bulk solution. Imagine that a fraction of the adsorbed chains is radioactively labeled. We denote their contribution to the total adsorbance by Γ^*. If the layer is exposed to a bulk solution containing only non-labeled chains, the exchange process in thermal equilibrium can be monitored experimentally. Since the overall adsorbance remains constant, we have

$$J_{ex} = J_{out} = J_{in} \sim \frac{k_B T}{\zeta_0} \phi_0 N^{-(2-\gamma_{2D}+\nu)} ,$$

and the adsorbance of the labeled chains decreases according to [25]

$$\frac{d\Gamma^*}{dt} = -J_{ex} \frac{\Gamma^*}{\Gamma} . \quad (23)$$

Therefore, J_{ex} defines the time scale of the exchange process by

$$\tau_{ex} = \frac{\Gamma}{J_{ex}} \sim \frac{\zeta_0}{\phi_0 k_B T} N^{2-\gamma_{2D}+\nu} . \quad (24)$$

Note that both time scales, τ_a and τ_{ex}, are inversely proportional to ϕ_0, and that the exchange time is larger than the adsorption time,

$$\frac{\tau_{ex}}{\tau_a} \sim N^{2\nu-1} .$$

as also found for the saturated layer in reference [25].

3 Exchange regime and growth regime

For the reminder of the paper, we consider a bidisperse mixture of short and long chains with masses N_1 and N_2, respectively. We assume that both types of chains have the same bulk concentration ϕ_0, that $N_1 > N_2$, and that the short chains remain strongly absorbed. The latter assumption implies that $N_2 > G$, which holds even at final equilibrium, provided $\Gamma_{2,eq} \geq \phi_0 N_2^{\gamma_{2D}-\gamma} G^{\gamma-\nu}/C$ (see Eq. (6)). Since the equilibrium structure of the bidisperse layer is dominated by long chains [1,22,23], we choose as initial condition a layer which mainly consists of short chains. The aim of this study is to describe the dynamics of the replacement process of short by long chains during the approach towards equilibrium.

Using the undersaturation X (see Eq. (19)) we write quite generally

$$K \sim X^{-\mu} \quad \text{and} \quad X \sim G^{-1/\delta} \quad (25)$$

with $\delta = 1/(2\nu-1) \approx 5.6$ and $\mu = (2-\gamma_{2D}+\nu)/(2\nu-1) \approx 7.8$ when excluded volume exponents and the Rouse-Zimm dynamics are used. The adsorption kinetics of a bidisperse solution is described by the rate equations

$$\frac{d\Gamma_i}{dt} = J_{in,i} - J_{out,i} \quad \text{for} \quad i = 1, 2 .$$

This yields with equations (16, 17)

$$\frac{d\Gamma_i}{dt} = \frac{k_B T}{\zeta_0} X^{\mu} \left[\phi_0 - C\Gamma_i N_i^{\gamma-\gamma_{2D}} X^{\alpha} \exp(-N_i X^{\delta})\right] \quad \text{for} \quad i = 1, 2 , \quad (26)$$

where $\alpha = \delta(\gamma - \nu)$ (≈ 3.2).

In the following we discuss equation (26) without specifying the value of the exponents. The qualitative picture that emerges thus mainly relies on the local equilibrium assumption (determining the general structure of the rate equations) and can accommodate slight changes otherwise (α and δ depend on chain statistics, whereas the relevant dynamics and the limiting process enter in μ). Furthermore, we restrict our analysis to the time range, in which the outward flux of the long chains, $J_{out,1}$, can be neglected. Since $J_{out,1}$ is related to the desorption of the strongly absorbed long chains, the flux is small from early up to late times close to the final saturation. This last stage could be studied by linearizing the rate equations around the thermodynamic equilibrium. When neglecting $J_{out,1}$, the explicit N_1 dependence in equation (26) drops out, and the variables are conveniently rescaled by N_2. Introducing the reduced variables

$$\tilde{\Gamma}_2 = \Gamma_2 N_2^{1/\delta} , \quad \tilde{X} = X N_2^{1/\delta} ,$$
$$\tilde{t} = \frac{t}{\tau_{a,2}} , \quad \tau_{a,2} = \frac{\zeta_0}{\phi_0 k_B T} N_2^{(\mu-1)/\delta} , \quad (27)$$
$$\tilde{\phi} = \frac{\phi_0}{\phi_2^\star} , \quad \phi_2^\star = C N_2^{1-\nu-\gamma_{2D}} ,$$

we write the rate equations as

$$\frac{d\tilde{\Gamma}_2}{d\tilde{t}} = \tilde{X}^{\mu} \left[1 - \tilde{\phi}^{-1} \tilde{\Gamma}_2 \tilde{X}^{\alpha} \exp(-\tilde{X}^{\delta})\right] \quad (28)$$

and

$$\frac{d\tilde{X}}{d\tilde{t}} = -\tilde{X}^{\mu} \left[2 - \tilde{\phi}^{-1} \tilde{\Gamma}_2 \tilde{X}^{\alpha} \exp(-\tilde{X}^{\delta})\right] . \quad (29)$$

The typical concentration $\phi_2^\star$ is only linked to equilibrium properties. Inserting excluded volume exponents we find that it is roughly proportional to the overlap concentration of the short chains. The time $\tau_{a,2}$ is the adsorption time of the short chains (see Eq. (22)). In our approach it is the shortest time scale of the adsorption kinetics and is therefore used as the time unit.

Eliminating the time variable, the rate equations connect the composition (or Γ_2) to the undersaturation *via*

$$\frac{d\tilde{X}}{d\tilde{\Gamma}_2} = -\frac{2 - \tilde{\phi}^{-1} \tilde{\Gamma}_2 \tilde{X}^{\alpha} \exp[-\tilde{X}^{\delta}]}{1 - \tilde{\phi}^{-1} \tilde{\Gamma}_2 \tilde{X}^{\alpha} \exp[-\tilde{X}^{\delta}]} . \quad (30)$$

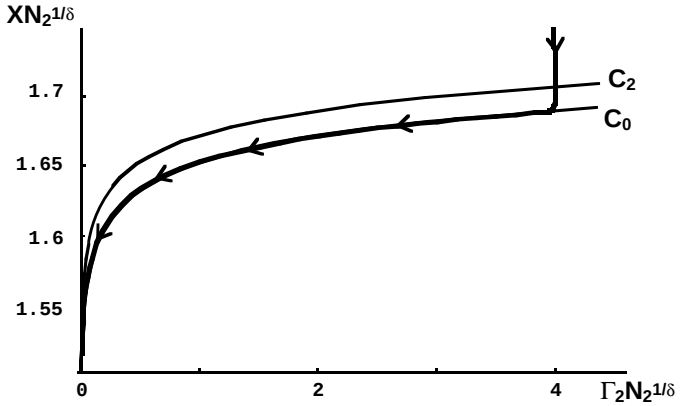

Fig. 1. Comparison of a typical flux line (thick solid line with arrows), $\tilde{X}(\tilde{\Gamma}_2)$, with the lines $\mathcal{C}_0$ (line of maximum undersaturation $\tilde{X}$) and $\mathcal{C}_2$ (line of maximum $\tilde{\Gamma}_2$), see equation (31). The flux line is calculated from the numerical solution of equation (30) using $\tilde{\phi} = 10^{-5}$, $\alpha = 3$ and $\delta = 5$ (the values of α and δ are obtained with the Flory estimate $\nu \approx 0.6$). Note that $\tilde{X}(\tilde{\Gamma}_2)$ is very close to $\mathcal{C}_0$.

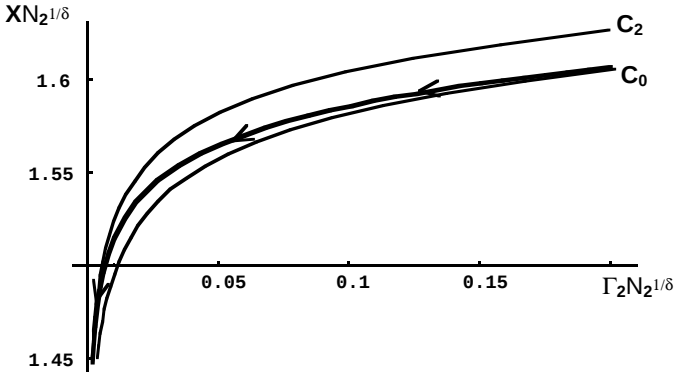

Fig. 2. Enlargement of the crossover region from Figure 1, where the flux line starts to deviate markedly from $\mathcal{C}_0$ and crosses over to $\mathcal{C}_2$. Note, however, that the line $\mathcal{C}_2$ is never reached in our approach due to the absence of the outward flux of the long chains.

In the $(\tilde{X},\tilde{\Gamma}_2)$-plane the competitive adsorption process is represented by a point which follows a flux line satisfying equation (30). There are two special lines in the plane: the lines $\mathcal{C}_0$ and $\mathcal{C}_2$, where respectively $\tilde{X}$ and $\tilde{\Gamma}_2$ are stationary and go through a maximum

$$\begin{aligned} \mathcal{C}_0: \quad & \tilde{\Gamma}_2 = 2\tilde{\phi}\tilde{X}^{-\alpha}\exp[\tilde{X}^{\delta}] \\ \text{and} \quad \mathcal{C}_2: \quad & \tilde{\Gamma}_2 = \tilde{\phi}\tilde{X}^{-\alpha}\exp[\tilde{X}^{\delta}]\,. \end{aligned} \tag{31}$$

In the vicinity of $\mathcal{C}_0$ the total adsorbance varies slowly, whereas the partial adsorbance of the short chains varies slowly in the vicinity of $\mathcal{C}_2$. Both lines exhibit an extremum at $\tilde{X}_e = (\alpha/\delta)^{1/\delta}$, where the prefactor, $\tilde{X}^{-\alpha}$, begins to dominate over the exponential for smaller $\tilde{X}$. However, this wing of the lines for small $\tilde{X}$ is not physical, since it violates the condition that the small chains are strongly adsorbed (*i.e.*, the condition $N_2 > G$).

A typical flux line for a system which is initially starved for both short and long chains is shown in Figure 1 together with $\mathcal{C}_0$ and $\mathcal{C}_2$. The undersaturation first drops sharply, whereas $\tilde{\Gamma}_2$ smoothly passes through its maximum on $\mathcal{C}_2$. The flux line approaches $\mathcal{C}_0$ from above without reaching it (remember that $\mathcal{C}_0$ is a line of maxima for the undersaturation). Then the total composition varies slowly, whilst the short chain content drops. The distance between the representative point and $\mathcal{C}_0$, measured by $\tilde{f}(\tilde{\Gamma}_2) = \tilde{X}(\tilde{\Gamma}_2) - \tilde{X}_0(\tilde{\Gamma}_2)$, where the last term corresponds to the curve $\mathcal{C}_0$, goes through a (very weak) minimum. The line of minima $\mathcal{C}_m$, defined by $d\tilde{f}/d\tilde{\Gamma}_2 = 0$ (see Eq. (A.1)), lies very closely above $\mathcal{C}_0$ and slightly separates from $\mathcal{C}_0$ with decreasing $\tilde{\Gamma}_2$. The flux line $\tilde{X}(\tilde{\Gamma}_2)$ crosses $\mathcal{C}_m$ only once, and then, being located in the narrow gap between $\mathcal{C}_0$ and $\mathcal{C}_m$, stays very close to $\mathcal{C}_m$ afterwards (the difference is never noticeable on the scale of the figure). The system thus evolves at almost constant undersaturation.

Physically, this means that short chains are replaced by longer ones until a situation is reached, where the vast majority of them is desorbed. In this "exchange regime" the layer nearly preserves its original thickness because almost stoichiometric amounts of the short chains are substituted. Note that the resulting layer, if considered as a layer of long chains, is severely undersaturated.

At lower values of $\tilde{\Gamma}_2$ both $\mathcal{C}_m$ and the (nearby) flux line depart from $\mathcal{C}_0$, and the layer begins to grow sharply (in the numerical example of Fig. 1 this happens at $\tilde{\Gamma}_2 < 0.1$, see Fig. 2). After a crossover regime ($\Gamma_2 < \Gamma_{2,co}$, see Eq. (33)) the flux line approaches $\mathcal{C}_2$ without reaching it (remember that it is a line of maxima for Γ_2). We call this regime the "growth regime". Here, the short chain content varies smoothly, whereas the total adsorbance grows rapidly. The line $\mathcal{C}_2$ would be reached if $J_{out,1}$ were included to describe the approach to the final equilibrium state of the layer (this would add a stable fixed point in the diagram. Nonetheless, the approach toward the fixed point is governed by the attractor for a system starting in the high $\tilde{\Gamma}_2$-region).

As discussed above, a flux line crossing $\mathcal{C}_m$ in the high $\tilde{\Gamma}_2$-region ($\Gamma_2 > \Gamma_{2,co}$) remains very close to $\mathcal{C}_m$ afterwards, and $\mathcal{C}_m$ itself is fairly close to $\mathcal{C}_0$. If one writes

$$\tilde{X} = \tilde{X}_0 + \tilde{f} = \tilde{X}_0 + \tilde{f}_m - \tilde{\eta}\,,$$

where $\tilde{f}_m$ is obtained from the solution of $d\tilde{f}/d\tilde{\Gamma}_2 = 0$, it can be shown that the correction, $\tilde{\eta}(\tilde{\Gamma}_2)$, quickly becomes independent of the flux line for decreasing $\tilde{\Gamma}_2$. Here, we give a brief proof by expanding $\tilde{X}$ around $\tilde{X}_0$ (for details see Appendix). In the exchange regime we find

$$\begin{aligned} \tilde{f}_{m,ex}(\tilde{X}_0) &= \frac{1}{2\tilde{\Gamma}_2}\frac{\tilde{X}_0^2}{\left(\delta\tilde{X}_0^{\delta} - \alpha\right)^2} \\ \tilde{\eta}(\tilde{\Gamma}_2) &= \int_{\tilde{\eta}=0}^{\tilde{\Gamma}_2} d\tilde{f}_{m,ex}(\tilde{\Gamma}_2') \\ &\quad \times \exp\left[-\int_{\tilde{\Gamma}_2}^{\tilde{\Gamma}_2'} d\tilde{\Gamma}_2''\frac{2(\delta\tilde{X}_0^{\delta} - \alpha)}{\tilde{X}_0}\right] \end{aligned} \tag{32}$$

where $\tilde{f}_{m,ex}$ denotes the approximate solution of $d\tilde{f}/d\tilde{\Gamma}_2 = 0$ for small $\tilde{f}$ (index "ex"), and $\tilde{\eta}(\tilde{\Gamma}_2)$ is obtained by integration of equation (A.3). The numerical examples illustrate two general features of the exchange regime: (1.) Since $\tilde{X}_0$ changes only slightly with decreasing $\tilde{\Gamma}_2$, the essential variation of $\tilde{f}_{m,ex}$ comes from $1/\tilde{\Gamma}_2$. (2.) The interval, $\Delta\tilde{\Gamma}_2 \sim \tilde{X}_0/(2[\delta\tilde{X}_0^\delta - \alpha])$, over which the exponential kernel entering $\tilde{\eta}$ decays, is small. Therefore $\tilde{\eta}/\tilde{f}_{m,ex}$ is of the order of $\sim (1/\tilde{f}_{m,ex})(d\tilde{f}_{m,ex}/d\tilde{\Gamma}_2)\Delta\tilde{\Gamma}_2 \sim \Delta\tilde{\Gamma}_2/\tilde{\Gamma}_2$, which is the relative deviation of the expanded $\tilde{f}_{m,ex}$ from $\mathcal{C}_m$. As long as $\Delta\tilde{\Gamma}_2/\tilde{\Gamma}_2 \ll 1$, the flux line stays close to $\mathcal{C}_0$ and belongs to the exchange regime. On the other hand, if $\Delta\tilde{\Gamma}_2/\tilde{\Gamma}_2 \gg 1$, it strongly deviates from $\mathcal{C}_0$ and is in the growth regime. Therefore the threshold, $\Delta\tilde{\Gamma}_2/\tilde{\Gamma}_2 = 1$, can be defined as the crossover to the growth regime, *i.e.*,

$$\tilde{\Gamma}_{2,co} = \frac{\tilde{X}_0^{1-\delta}}{2\delta} \ . \tag{33}$$

The variation of $\Delta\tilde{\Gamma}_2$ is smooth over the exchange regime, where it is everywhere of order $\tilde{\Gamma}_{2,co}$. Thus the actual flux line hardly depends on values of $\tilde{\Gamma}_2'$ larger than $\tilde{\Gamma}_2 + \tilde{\Gamma}_{2,co}$. The flux line after crossing $\mathcal{C}_m$ becomes universal and is very close to $\mathcal{C}_m$, once $\tilde{\Gamma}_2$ has decreased by $\sim \tilde{\Gamma}_{2,co}$.

In the growth regime the flux line closely approaches $\mathcal{C}_2$ from below, but never reaches it because we omitted the outward flux of the long chains. Writing therefore $\tilde{X} = \tilde{X}_2 - \tilde{g}(\tilde{\Gamma}_2)$ and expanding for small $\tilde{g}$ we obtain (see Appendix)

$$\tilde{X} = \tilde{X}_2 - \tilde{\Gamma}_2 + cst \times \exp\left[-\int_{\tilde{\Gamma}_2}^{\tilde{\Gamma}_{2,co}} d\tilde{\Gamma}_2 \frac{\tilde{X}_2}{\tilde{\Gamma}_2^2\left(\delta\tilde{X}_2^\delta - \alpha\right)}\right] , \tag{34}$$

where the constant is of the order of the deviation from $\tilde{X}_0$ in the crossover region. The integral can be safely neglected in the growth regime up to $\tilde{\Gamma}_{2,co}$. A more precise description of the universal flux line is not needed.

The adsorption kinetics is given by the kinematics of the representative point on its flux line. In the following we restrict ourselves to the universal part of the flux line, leaving the initial regime and the final saturation for future work, and we work only with the leading order approximations for the flux line, *i.e.*, with $\tilde{X} \simeq \tilde{X}_0 + \tilde{f}_{m,ex}$ and $\tilde{X} \simeq \tilde{X}_2 - \tilde{\Gamma}_2$ in the exchange and growth regime, respectively. A direct comparison of these approximations with the flux line obtained from the numerical solution is given in Figure 3. The integration of the kinetic equations (28, 29) is then straightforward. Taking the time origin at the crossing of the flux line with $\mathcal{C}_m$ and inserting $\mathcal{C}_0$ in the right hand side of equation (28) the exchange kinetics for Γ_2 obeys

$$\Gamma_2(t) \simeq \Gamma_2(0) - \frac{t}{\tau_{ex,2}}\tilde{X}^\mu \ , \tag{35}$$

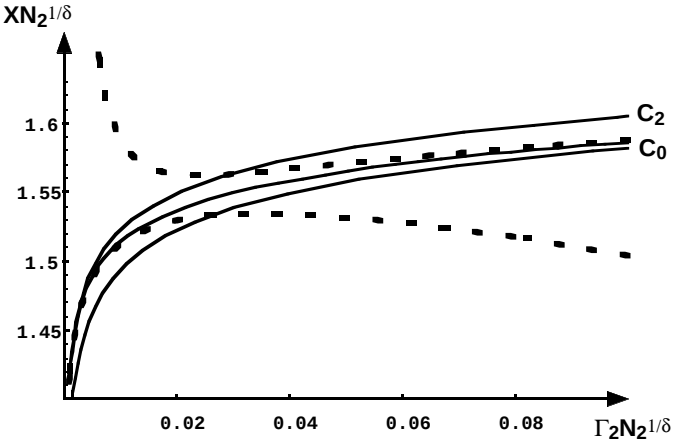

Fig. 3. Comparison of the numerical solution for the flux line (Eq. (30)) with the approximate analytical formulas (dashed lines) $\tilde{X} = \tilde{X}_0 + \tilde{f}_{m,ex}$ (exchange regime) and $\tilde{X} = \tilde{X}_2 - \tilde{\Gamma}_2$ (growth regime). The same parameters as in Figure 1 were used. In addition, the characteristic lines $\mathcal{C}_0$ and $\mathcal{C}_2$ are shown.

where $\tau_{ex,2}$ denotes the exchange time of the short chains and is given by (see also Eq. (24))

$$\tau_{ex,2} = \frac{\zeta_0}{\phi_0 k_B T} N_2^{\mu/\delta} \ . \tag{36}$$

To obtain equation (35) the slow variation of $\tilde{X}$ (see Eq. (38)) was neglected during the integration. If $\tilde{X}$ is taken equal to $\tilde{X}(0)$, an approximate linear time dependence results for Γ_2.

Similarly, if we expand $\tilde{\Gamma}_2(\tilde{X})$ around $\tilde{X}_0$ and insert the result in the right hand side of equation (29) we obtain

$$\frac{t}{\tau_{a,2}} = -2\tilde{\phi}\int_{\tilde{X}^\delta(0)}^{\tilde{X}^\delta} du \frac{\exp[u]}{u^{(\mu+\alpha)/\delta}} \ , \tag{37}$$

which shows that

$$\tilde{X}^\delta \sim \ln\frac{t_0 - t}{\tau_{ex,2}} \ . \tag{38}$$

In the last step we assumed that the integrand of equation (37) is dominated by the exponential, and t_0 is an integration constant. Equations (35, 38) show that the thickness of the layer only varies logarithmically with time (see Fig. 4), whereas the composition decreases almost linearly in the exchange regime (see Fig. 5). These results qualitatively agree with the behavior found in the experiments on PEO [5]. For example, compare Figures 6 and 5 with the variation of the total and partial adsorbances given in references [5,20]. Additionally, from equation (35) and the condition $\Delta\Gamma_2 \approx \Gamma_2$ we see that the exchange regime typically lasts a time $t_{ex} \approx \tau_{ex,2}(\ln[\tilde{X}_0^\alpha/(2\tilde{\phi})])^{-\mu/\delta}$. This time is smaller than $\tau_{ex,2}$, which illustrates that the replacement process of the short by long chains is more efficient than that by a solution consisting of short chains only. It is a fast process in qualitative agreement with the experimental results for PEO.

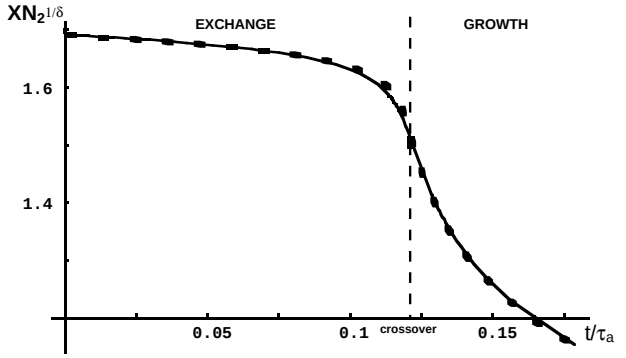

Fig. 4. Evolution of the undersaturation with $t/\tau_{a,2}$. The solid line is the numerical solution of equations (28, 29), using $\mu = 7$, $\alpha = 3$ and $\delta = 5$, whereas the dashed line shows the asymptotic solution equations (37, 39).

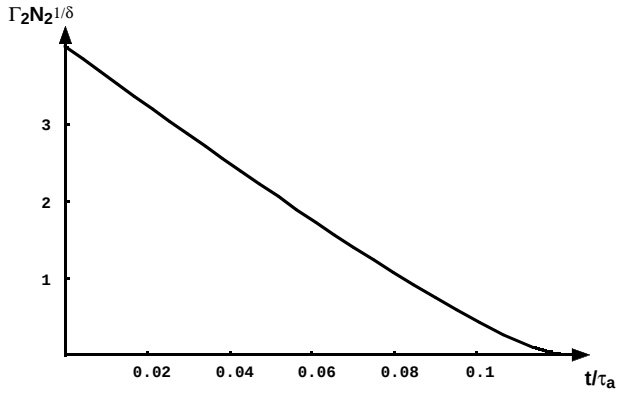

Fig. 5. Variation of the partial adsorbance of the short chains, Γ_2, as a function of time. The crossover to the growth regime is located at the very right of the figure ($t > 0.1\tau_{a,2}$). The same values for the parameters as in Figure 4 are used.

Using the leading approximation for the flux line in the growth regime, $\tilde{X} \approx \tilde{X}_2 - \tilde{\Gamma}_2$, we find from equation (29)

$$\frac{t - t_1}{\tau_{a,2}} \simeq \frac{1}{\mu - 1} \tilde{X}^{-(\mu-1)} \; . \tag{39}$$

Similarly, by expanding $\tilde{X}$ around $\tilde{X}_2$ and inserting equation (39) in equation (28) we obtain for the adsorbance of the small chains

$$\tilde{\Gamma}_2 \simeq c_1 \exp\left[\frac{(\mu-1)(t-t_1)}{\tau_{a,2}}\right]^{-\delta/(\mu-1)} \; . \tag{40}$$

The integration constants, t_1 and c_1, in these equations allow to match the growth with the exchange regime. The complete vanishing of $\tilde{\Gamma}_2$ at large times results from the neglect of $J_{out,1}$ in our theoretical description. In practice, it is always cut off by saturation effects (or by the weak adsorption regime of the short chains).

4 Conclusions

In this paper we have studied the competitive adsorption between long and short polymer chains in the regime

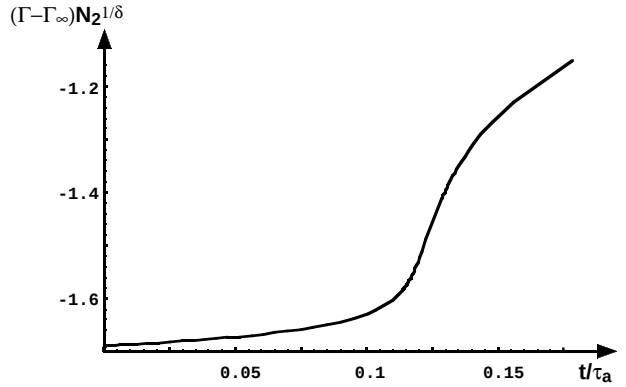

Fig. 6. The total adsorbance as a function of time. Same values for the parameters as in Figure 4.

of moderate chain length and high dilution (typically up to $\sim 10^3$ segments and $\phi_0 \ll \phi^*$). The internal equilibrium of the layer in contact with a bidisperse solution imposes a universal adsorption dynamics independent of the preparation of the layer. If $\Gamma_2 > \Gamma_{2,co}$, short chains are mainly exchanged by long chains. In this exchange regime Γ_2 decreases approximately linearly with time, whilst the layer thickness is roughly constant (logarithmic time dependence). In the subsequent growth regime the thickness increases as a power law until saturation sets in. This is in qualitative agreement with experimental results for poly(ethylene oxide) [5,24] that show some evidence for well separated exchange and growth regimes.

The internal equilibrium assumption is the main assumption of our theory. It amounts to assume that at any time the distribution of loops and tails corresponds to equilibrium under the instantaneous coverage constraint. From a formal point of view this is justified at low bulk concentration as the characteristic adsorption time is proportional to $1/\phi_0$.

Polymers are described by excluded volume statistics using scaling laws. This seems appropriate to obtain the structure of the rate equations and discuss robust features of the dynamics as we did. A mean-field theory can be worked out in more details at least for the isotherm. The growth problem itself is treated at a mean-field level, thereby the coupling between the dynamics of the penetrating chain and the local density fluctuations in the layer is neglected. This is to say that the slowly penetrating chain experiences the average concentration profile.

We used Rouse-Zimm dynamics throughout the whole analysis. Entanglements between chains can in practice play an important role. When this happens, the chains cannot freely explore all configurations, and the full partition function is not relevant. Entanglements are most likely to matter closest to the wall and thus during the spreading process. The description of the complex reptative motions close to the wall is beyond the scope of this paper. However, any topological constraint would increase the resistance opposed by the layer to chain penetration and thus favor control by the layer compared with control by bulk diffusion. A stronger dependence of the resistance on the layer thickness is then anticipated.

As our discussion of the kinetic equations can accommodate higher values of the exponent μ measuring the layer resistance, the existence of well separated exchange (here μ only appears in the power of a logarithm) and growth regimes that mainly relies on the local equilibrium assumption seems robust against changes in the chain dynamics.

Our theory does not apply to the case of strongly binding monomers where no exchange, or only partial exchange, is expected over experimental time scales. The system gets trapped in various metastable states depending on its preparation. For example, incoming chains can bridge over preadsorbed chains and pin them on the surface [30]. The local equilibrium assumption, which determines the physics in our approach, then fails. It was also assumed that spreading is achieved by in-plane flow of the monomers, as is reasonable for weakly binding monomers (or without site-binding on an in-plane structure). If the flow is hindered by strong site-binding of the monomers, it may be faster for the incoming chain to explore the surface for empty sites by diffusion.

Appendix: Approximate solutions for the flux line

We start from equation (30) and write $\tilde{X} = \tilde{X_0} + \tilde{f}$, where $\tilde{f}$ will be taken as an expansion parameter in the vicinity of $\mathcal{C}_0$. By definition (see Eqs. (30, 31)) the function $\tilde{f}$ satisfies the following differential equation

$$\frac{d\tilde{f}}{d\tilde{\Gamma}_2} = -1 - \frac{1}{1-\tilde{\phi}^{-1}\tilde{\Gamma}_2\tilde{X}^\alpha \exp[-\tilde{X}^\delta]} - \frac{\tilde{X}_0}{\tilde{\Gamma}_2(\delta\tilde{X}_0^\delta - \alpha)} \,. \quad \text{(A.1)}$$

The right hand side vanishes on the line $\mathcal{C}_m$ which is the envelope of the closest approach of the various flux lines, $\tilde{X}(\tilde{\Gamma}_2)$, (coming from above) to $\mathcal{C}_0$. This gives an implicit equation for $\mathcal{C}_m$. It can be shown that the universal flux line follows $\mathcal{C}_m$ closely everywhere (in the case corresponding to the figures the difference is 1/1000 in the cross over region and much less otherwise; qualitatively, this is shown in Fig. 7). Here, we restrict ourselves to an expansion for small $\tilde{f}$, which holds in the exchange regime. Expanding for $\delta\tilde{X}_0^{\delta-1}\tilde{f} \ll 1$ and inserting $\tilde{\Gamma}_2$ as a function of $\tilde{X}_0$ (*i.e.*, Eq. (31)) we find

$$\frac{d\tilde{f}_{ex}}{d\tilde{\Gamma}_2} = \frac{2\left(\delta\tilde{X}_0^\delta - \alpha\right)}{\tilde{X}_0}\tilde{f}_{ex} - \frac{\tilde{X}_0}{\tilde{\Gamma}_2\left(\delta\tilde{X}_0^\delta - \alpha\right)} \,,$$

where the index "ex" denotes an expansion for small $\delta\tilde{X}_0^{\delta-1}\tilde{f}$. The derivative vanishes if

$$\tilde{f}_{m,ex} = \frac{\tilde{X}_0^2}{2\tilde{\Gamma}_2\left(\delta\tilde{X}_0^\delta - \alpha\right)^2} \,, \quad \text{(A.2)}$$

which shows that $\delta\tilde{X}_0^{\delta-1}\tilde{f}_{m,ex} \simeq \tilde{X}_0^{1-\delta}/(2\delta\tilde{\Gamma}_2)$. Therefore the expansion holds down to the crossover $\tilde{\Gamma}_{2,co} = \tilde{X}_0^{1-\delta}/2\delta$ (see Eq. (33)).

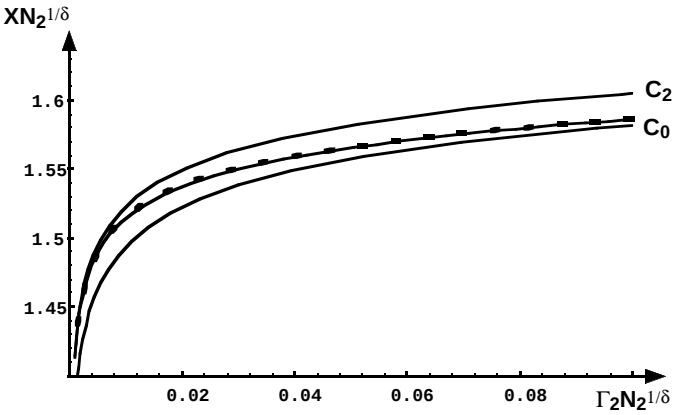

Fig. 7. Comparison of the numerical solution for the flux line (Eq. (30)) with the true (unexpanded) line $\mathcal{C}_m$ (dashed). The same parameters as in Figure 1 are used. In addition, the characteristic lines $\mathcal{C}_0$ and $\mathcal{C}_2$ are shown.

The deviation of the flux line from $\mathcal{C}_m$, $\tilde{\eta} = \tilde{f}_{m,ex} - \tilde{f}$, satisfies

$$\frac{d\tilde{\eta}}{d\tilde{\Gamma}_2} = \frac{2(\delta\tilde{X}_0^\delta - \alpha)}{\tilde{X}_0}\tilde{\eta} + \frac{d\tilde{f}_{m,ex}}{d\tilde{\Gamma}_2} \,. \quad \text{(A.3)}$$

The integration of the last equation leads to equation (32) in the main text.

Similarly, one can proceed in the growth regime, where $\tilde{X}$ closely approaches $\tilde{X}_2$ from below. Writing therefore $\tilde{X} = \tilde{X}_2 - \tilde{g}$ we obtain from equations (30, 31) the differential equation

$$\frac{d\tilde{g}}{d\tilde{\Gamma}_2} = 1 + \frac{1}{1-\tilde{\phi}^{-1}\tilde{\Gamma}_2\tilde{X}^\alpha \exp[-\tilde{X}^\delta]} + \frac{\tilde{X}_2}{\tilde{\Gamma}_2(\delta\tilde{X}_2^\delta - \alpha)}, \quad \text{(A.4)}$$

which yields, when using $\tilde{g}$ as a small parameter,

$$\frac{d\tilde{g}}{d\tilde{\Gamma}_2} = 1 + \frac{\tilde{X}_2}{(\delta\tilde{X}_2^\delta - \alpha)}\left[\frac{1}{\tilde{\Gamma}_2} - \frac{1}{\tilde{g}}\right] \,. \quad \text{(A.5)}$$

An obvious solution of this equation is $\tilde{g} = \tilde{\Gamma}_2$. To remove the apparent singularity at low $\tilde{\Gamma}_2$, we expand equation (A.5) in the difference $\tilde{\varepsilon} = \tilde{g} - \tilde{\Gamma}_2$. Integration of the resulting expression yields equation (34) of the main text. It can be checked *a posteriori* that $\tilde{\varepsilon}$ has to be small in order to match the exchange and the growth regimes at the crossover.

A direct expansion around the exact $\mathcal{C}_m$ confirms that the flux line is indeed very close to $\mathcal{C}_m$ everywhere. It can also be checked directly that the lines $\tilde{X}_0 - \tilde{f}_{m,ex}$ and $\tilde{X}_2 - \tilde{\Gamma}_2$ merge with $\mathcal{C}_m$ from above and below the crossover, respectively.

References

1. G.J. Fleer, M.A. Cohen Stuart, J.M.H.M. Scheutjens, T. Cosgrove, B. Vincent, *Polymers at Interfaces* (Chapman & Hall, London, 1993).
2. I.C. Sanchez, *Physics of Polymer Surfaces and Interfaces* (Butterworth-Heinemann, Boston, 1992).
3. H.M. Schneider, P. Frantz, S. Granick, Langmuir **12**, 994 (1996).
4. E. Pefferkorn, A. Haouam, R. Varoqui, Macromol. **22**, 2677 (1989).
5. J.C. Dijt, M.A. Cohen Stuart, G.J. Fleer, Macromol. **27**, 3219 (1994).
6. J.F. Douglas, H.M. Schneider, P. Frantz, R. Lipman, S. Granick, J. Phys.-Cond. **9**, 7699 (1997).
7. H.M. Schneider, S. Granick, S. Smith, Macromol. **27**, 4714 (1994); *ibid.*, 4721.
8. S. Granick, in *Physics of Polymer Surfaces and Interfaces*, edited by I.C. Sanchez (Butterworth-Heinemann, Boston, 1992), pp. 227–244.
9. O. Guiselin, Europhys. Lett. **17**, 225 (1992).
10. L.-C. Jia, P.-Y. Lai, J. Chem. Phys. **105**, 11319 (1996).
11. P.-G. de Gennes, Adv. Colloid Interface Sci. **27**, 189 (1987).
12. A.N. Semenov, J. Bonet-Avalos, A. Johner, J.-F. Joanny, Macromol. **29**, 2179 (1996).
13. A. Johner, J. Bonet-Avalos, C.C. van der Linden, A.N. Semenov, J.-F. Joanny, Macromol. **29**, 3629 (1996).
14. J.F. Douglas, P. Frantz, H.E. Johnson, H.M. Schneider, S. Granick, Colloids and Surfaces A: Physicochemical and Engineering Aspects **86**, 251 (1994).
15. H.E. Johnson, J.F. Douglas, S. Granick, Phys. Rev. Lett. **70**, 3267 (1993).
16. E. Bouchaud, M. Daoud, J. Phys. France **48**, 1991 (1987).
17. M. Aubouy, O. Guiselin, E. Raphael, Macromol. **29**, 7261 (1996).
18. P.-G. de Gennes, C.R. Acad. Sci. (Paris) II **294**, 1317 (1982).
19. E. Pefferkorn, A. Carroy, R. Varoqui, J. Polymer Sci. Polymer Phys. **23**, 1997 (1985).
20. M.A. Cohen Stuart, M.C.P. van Eijk, J.C. Dijt, H.G. Hoogeveen, Macromol. Symp. **113**, 163 (1997).
21. M.A. Cohen Stuart, G.J. Fleer, in *Annual Reviews of Materials Science*, edited by M. Tirell, E.N. Kaufmann, J.A. Giordmaine, J.B. Wachtman, (Annual Reviews Inc., Palo Alto, 1996), Vol. 26, pp. 463-500.
22. G.J. Fleer, Colloids and Surfaces A: Physicochemical and Engineering Aspects **104**, 271 (1995).
23. J. Baschnagel, A. Johner, J.-F. Joanny, Phys. Rev. E **55**, 3072 (1997).
24. M. Santore, F. Fu, Macromol. **30**, 8516 (1997).
25. A.N. Semenov, J.-F. Joanny, J. Phys. II France **5**, 859 (1995).
26. E. Eisenriegler, *Polymers near Surfaces* (Clarendon Press, Singapore, 1993).
27. A.N. Semenov, J.-F. Joanny, Europhys. Lett. **29**, 279 (1995).
28. B. Duplantier, J. Stat. Phys. **54**, 581 (1989).
29. G. Fleer, Macromol. Symp. **113**, 177 (1997).
30. H.E. Johnson, S.S. Granick, Science **255**, 966 (1992).